UDC 519.6 **DOI: 10.20998/2222-0631.2025.02(9).13**

V. S. OVERKO

THE INFLUENCE OF THE TORSION MOTION OF LEFT VENTRICLE (LV) ON FEATURES OF BLOOD FLOW

The torsional motion (or twisting) of the left ventricle (LV) plays a crucial role in the ejection and filling of the left ventricle. During the cardiac cycle, systolic twisting and early diastolic untwisting of the left ventricle occurs around its long axis due to oppositely directed apical and basal rotations. From the apex of the LV, the systolic apical rotation occurs counterclockwise, while the basal rotation occurs clockwise. The size and characteristics of this torsional deformation have been described in various clinical and experimental studies, and it is well established that LV rotation is sensitive to changes in both regional and global LV function. Therefore, the assessment of LV rotation represents an interesting approach for the quantitative evaluation of LV function. Understanding blood flow patterns in the heart has numerous applications in hemodynamic analysis and clinical assessment of heart function. This study presents numerical simulations of blood flow in an idealized model of the left ventricle (LV) and the aortic sinus. The movement of the walls of the LV and aortic sinus was obtained from the analysis of kinematic images from MRI and used as constraints for the numerical computational fluid dynamics (CFD) model based on the moving boundary approach. The simulation results include detailed flow characteristics such as velocity, pressure, and wall shear stress for the entire volume. Additionally, to model the behavior of fluid flow within the human left ventricle, it is essential to consider the influence of non-Newtonian behavior of blood on numerical predictions throughout the entire cardiac cycle. Experimental studies indicate that blood significantly exhibits behavior associated with non-Newtonian properties in diseases such as myocardial infarction, cerebrovascular diseases, and hypertension; thus, the rheology of blood should be incorporated into numerical modeling of cardiovascular systems. Furthermore, due to recent advancements in CFD modeling, it has become easier to implement complex non-Newtonian assumptions into the Navier-Stokes equations. This article analyzes the impact of the torsional motion of the walls of the human left ventricle on the characteristics of blood circulation in the LV chamber and the initial section of the aorta. Non-Newtonian effects were considered using the Carreau-Yasuda model. This model describes blood as a non-Newtonian fluid with finite Newtonian states corresponding to a constant viscosity value. It is important to note that this model representation aligns well with experimental data.

Key words: left ventricle, torsion motion, blood flow, computer simulation, blood flow, pressure fields, velocity fields, cardiac cycle, second-order accuracy difference scheme, upwinding scheme.

В. С. ОВЕРКО

ВПЛИВ ТОРСІЙНОГО РУХУ ЛІВОГО ШЛУНОЧКА (ЛШ) НА ОСОБЛИВОСТІ КРОВООБІГУ

Торсійний рух (або скручування) лівого шлуночка (ЛШ) відіграє важливу роль у відношенні до викиду та наповнення лівого шлуночка. Протягом серцевого циклу спостерігається систолічне скручування та раннє діастолічне розкручування ЛШ навколо його довгої осі через протилежно спрямовані апікальні та базальні обертання. Зі сторони апексу ЛШ, систолічне апікальне обертання відбувається проти годинникової стрілки, а базальне обертання – за годинниковою стрілкою. Розмір і характеристики цієї торсійної деформації були описані в різних клінічних та експериментальних дослідженнях, і добре встановлено, що обертання ЛШ чутливе до змін як регіональної, так і глобальної функції ЛШ. Тому оцінка обертання ЛШ представляє собою цікавий підхід для кількісної оцінки функції ЛШ. Розуміння патернів кровотоку в серці має численні застосування в аналізі гемодинаміки та клінічній оцінці функції серця. У цьому дослідженні представлені чисельні симуляції кровотоку в ідеалізованій моделі лівого шлуночка та аортального синуса. Рух стінок ЛШ та аортального синуса отримано з аналізу кінематичних зображень МРТ і використано як обмеження для чисельної моделі обчислювальної гідродинаміки, основаної на підході рухомої межі. Результати симуляцій включають детальні характеристики потоку, такі як швидкість, тиск та зсув напруги стінок для всього об'єму. Також, щоб моделювати поведінку потоку рідини всередині лівого шлуночка серця людини (ЛШ), необхідно враховувати влив неньютоновської поведінки крові на чисельне прогнозування протягом всього серцевого циклу. Експериментальні дослідження свідчать, що кров значно демонструє поведінку, що пов'язана з неньютонівськими властивостями крові, у таких захворюваннях, як інфаркт міокарда, цереброваскулярні захворювання та гіпертонія; отже, реологічність крові слід застосовувати в чисельному моделюванні серцево-судинних систем. Крім того, внаслідок недавнього прогресу в комп'ютерній обчислювальній гідродинаміці тепер стало легше реалізувати складні неньютонівські припущення в рівняннях Нав'є – Стокса. У цій статті аналізується вплив торсійного руху стінок лівого шлуночка серця людини на характеристики кровообігу у камері ЛШ та в початковій ділянці аорти. Неньютонівські ефекти були враховані, використовуючи модель Карро – Ясуди. Ця модель описує кров як неньютонівську рідину з кінцевими ньютонівськими станами, що відповідають постійному значенню в'язкості. Важливо відзначити, що таке модельне представлення досить добре узгоджується з експериментальними даними.

Ключові слова: лівий шлуночок, торсійний рух, кровообіг, комп'ютерне моделювання, течія крові, поля тиску, поля швидкості, кардіальний цикл, різницева схема другого порядку точності, різниці проти потоку.

Introduction. Despite recent significant advancements in medicine, science, and technology, cardiovascular diseases remain one of the leading causes of mortality worldwide; thus, research aimed at assessing heart function is increasing daily. Previous studies have demonstrated that mechanical factors are closely linked to cardiovascular diseases. Therefore, understanding blood flow patterns in the heart has numerous applications in hemodynamic research and for the clinical assessment of heart function. For instance, this knowledge can be utilized in cardiac surgery and for the development of artificial hearts and heart valve prostheses.

Analysis of Recent Studies. The cardiac cycle consists of two main phases: the diastole and the systole. The first is the ventricular filling phase and the second is *the ventricular contraction phase*. *The LA* is located prior to *the LV* and therefore will serve as an inlet conduit for the LV. During a cycle the LA's function can be divided into three phases: the reservoir, conduit and contraction phase. The reservoir phase is during systole when the LA receives the oxygenated blood from the lungs through its *pulmonary veins (PVs)* and acts like a reservoir to the LV. The conduit phase is the passive emptying of the atrium due to the ventricular relaxation in the early diastole. The contraction phase occurs at the end of diastole when the LA contracts to re-increase the pressure and eject more blood into the ventricle. According to *Fyrenius* et al. [1], the normal LA has important roles in optimizing left ventricular filling. In vivo measurements indi-

cate that vortices develop in LA during the diastole before they disappear with atrial contraction. For the last decades, a few studies have concentrated on flow dynamics in the left atrium [1 – 3]. Hence, the understanding of the global flow pattern within the LA has remained yet unclear [1].

The left ventricular torsion (or twist) plays an important role with respect to LV ejection and filling [4 – 9]. In the cardiac cycle, there is a systolic twist and an early diastolic untwist of the LV around its long axis. This twist is caused by oppositely directed apical and basal rotations. Under consideration of the LV apex, we can observe the counterclockwise systolic apical rotation and the clockwise basal rotation. The characteristics of these torsional deformations have been described in different clinical and experimental investigations, where it was established that LV rotation is sensitive to local and global changes in LV. The left ventricular torsion caused by a motion of helically oriented miofibers is important to understanding the processes within the heart but difficult to measure. Ultrasound *speckle tracking imaging (STI)* is potentially suitable for measurement of angular motion because of its angle-independence [10]. The LV motion is shown on Fig. 1.

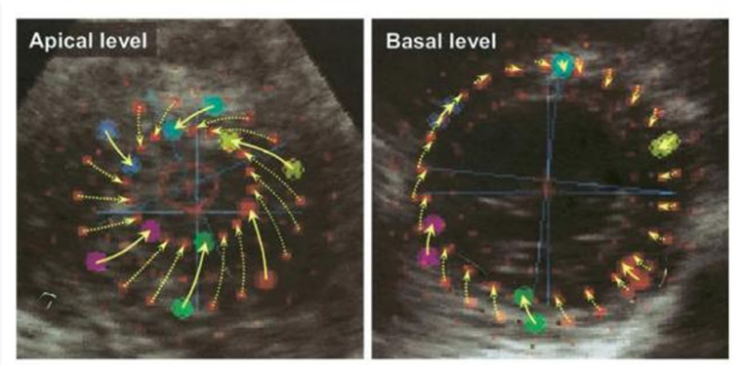

Fig. 1 – The Left ventricular rotation (LVrot) at apical and basal levels during systole by "overlaid" speckle tracking images [10].

End-systolic speckle tracking imaging acquisitions are overlaid at the end-diastolic image with corresponding local trajectories (the tail and the head of arrows indicate the location of end-diastole and end-systole). The LVrot was estimated from all of these regional angle displacements. Normally, on the apical level, the left ventricle rotates counterclockwise as viewed from apex, whereas the base rotates clockwise, as in this representative case. This gradient of LVrot between the two levels creates a «wringing» motion of the left ventricle [10].

MATERIALS AND METHODS. The full system of *Navier – Stokes equation* in three dimensional formulation was solved in unsteady laminar simulations using an implicit pressure-based solver. The pressure was calculated according to *the Standard scheme*. Concerning the pressure velocity coupling, the PISO scheme with *Skewness-Neighbor Coupling* was chosen. Momentum was discretized according to *Second Order Upwind scheme* [11].

The arterial wall was considered as rigid. This assumption is used in accordance with the results of [12, 13] which showed that shear stress values on the wall do not qualitatively and quantitatively differ practically in models using the approximation of rigid walls and elastic walls. This assumption has also made it possible to avoid using of source expensive *FSI algorithms*. For modeling *the non-Newtonian blood fluid* and the viscoelastic arterial wall *the Carreau model governed* by the following equation are used [14, 15, 16]:

$$\mu = \mu_\infty + \left(\mu_0 - \mu_\infty\right)\left(1 + \left(\lambda\dot{\gamma}\right)^2\right)^a, \tag{1}$$

$\mu_\infty = 0.056 Pa \cdot s$, the zero shear rate viscosity, $\mu_0 = 0.0036 Pa \cdot s$, the infinite shear rate viscosity, $\lambda = 3.313$, $a = 0.3568$.

System of governing equations:

$$\rho\left(\frac{\partial u}{\partial t} + u\frac{\partial u}{\partial y} + v\frac{\partial u}{\partial z} + w\frac{\partial u}{\partial z}\right) = -\frac{\partial P}{\partial x} + \mu\left(\frac{\partial^2 u}{\partial x^2} + \frac{\partial^2 u}{\partial y^2} + \frac{\partial^2 u}{\partial z^2}\right); \tag{2}$$

$$\rho\left(\frac{\partial v}{\partial t} + u\frac{\partial v}{\partial x} + v\frac{\partial v}{\partial z} + w\frac{\partial v}{\partial z}\right) = -\frac{\partial P}{\partial y} + \mu\left(\frac{\partial^2 v}{\partial x^2} + \frac{\partial^2 v}{\partial y^2} + \frac{\partial^2 v}{\partial z^2}\right); \tag{3}$$

$$\rho\left(\frac{\partial w}{\partial t} + u\frac{\partial w}{\partial y} + v\frac{\partial w}{\partial z} + w\frac{\partial w}{\partial z}\right) = -\frac{\partial P}{\partial z} + \mu\left(\frac{\partial^2 w}{\partial x^2} + \frac{\partial^2 w}{\partial y^2} + \frac{\partial^2 w}{\partial z^2}\right); \tag{4}$$

$$\frac{\partial u}{\partial x} + \frac{\partial v}{\partial y} + \frac{\partial w}{\partial z} = 0. \tag{5}$$

A parabolic velocity profile corresponding to the volumetric blood flow was used as spatial part of the inlet boundary condition.

Two wave of cardiac circle was performed. Results was given from second ones. This assumption was based on our test simulation of non-Newtonian blood flow in a direct tube for three cardiac cycles. This simulations indicated that differences are significant between the first and second cycle model results, with negligible differences between the second and subsequent cycles. A 0 mmHG pressure outlet condition with back flow specification method from neighboring cell was assigned at the outlet boundary for all models [17]. A no-slip condition was assumed at the wall.

Results. The pressure in a rotating body i.e. left ventricle decreases from rotating walls to a center of rotation. The pressure gradient imparts the necessary centripetal acceleration. The fluids admit a motion on a curved path. We simulate the blood flow in the two systolic.

Phase 1: The ventricular pressure exceeds the pressure in the aorta, the aortic valve opens and a rapid ejection of blood into the aorta starts. The ventricular muscles begin to shorten and the ventricular volume decreases. As seen from [18], the pressure gradient between the aorta and the LV is quite small. This is possible because of the relatively large aortic opening (i.e., *the low resistance*). As a result of LV contraction and shortening, the mitral ring descends and the LA expands slightly. Thus decreasing of LA pressure occurs. Venous blood continues to flow into the LA from the veins and the atrial pressure begins to rise again.

Phase 2: The period of the reduced ejection begins. The LV pressure decreases gradually and begins a bit less then the aortic pressure, which is also decreases as well. However, the blood continues to flow out of the LV due to the inertial effects. At the end of systole, the LV pressure vanishes faster and the blood begins to flow back towards the LV. The blood flows into the edges of the aortic valve close abruptly. The passive filling of the atrial chamber continues during this period and to the end of second phase [18, 19].

The field of pressure in the vertical plane of T-model is presented on the Fig. 2. In case of positive rate and acceleration of flow at the begin of systole (Fig. 2, *A*) the pressure is decreasing from the apex to the aorta. We can observe two zones with small pressure in the root of the aorta. These zones can be associated with the thorus-like vortex. The mechanism of appearance of this vortex is similar to the vortex at the backward step. When the velocity is maximal (Fig. 2, *B*) the pressure field has more complex form. A basal zone has higher pressure than central, apical and aortic root parts. Separated zones loss a symmetric form. In the case of the negative acceleration of flow at the end of systole (Fig. 2, *C*), the pressure of the apical part of left ventricle is less than the pressure of the central one. This effect caused by the torsion motion where the velocity of a wall is more than one in the central part of the left ventricle. At the end of the systole (Fig. 2, *D*) the pressure doesn't have singularities and increases from the apex to the aortic part. Now the left ventricle is ready for filling in the diastolic part of the cardiac circle.

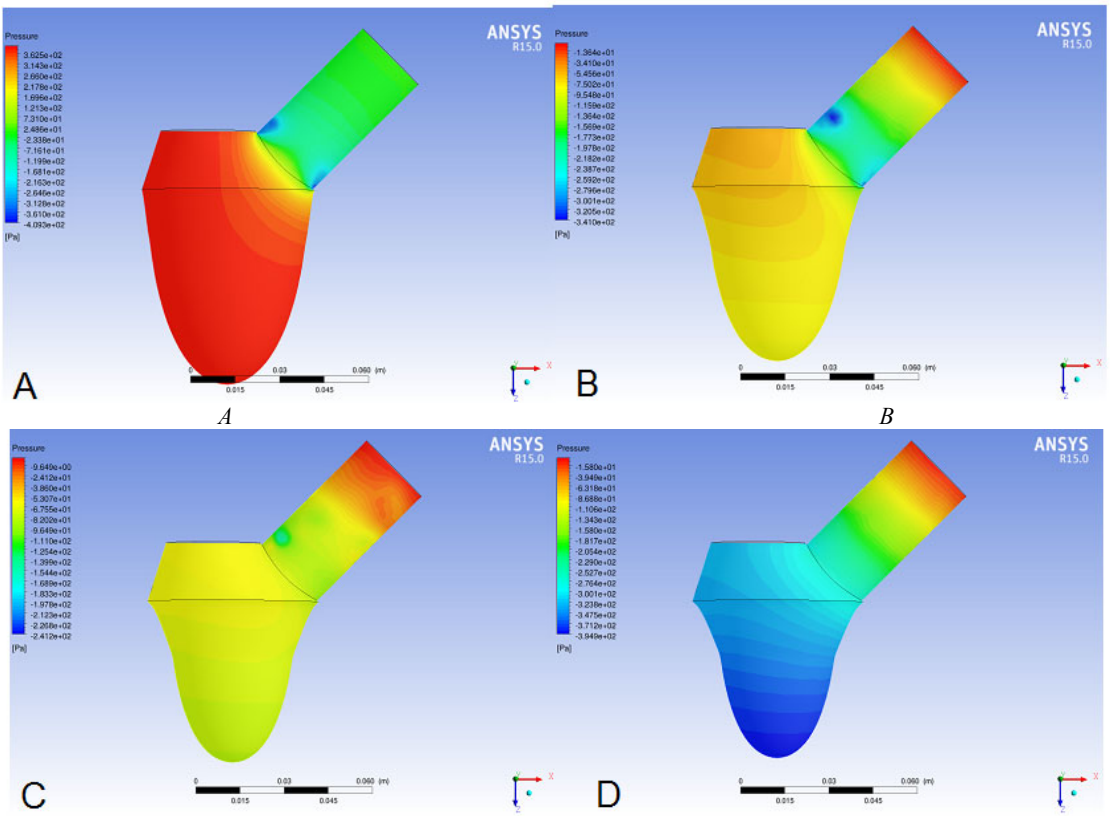

A *B*

C *D*

Fig. 2 – The pressure at the vertical cross plane for UT-models in the different time: *A* – time $= 0.07\,\text{s}$; *B* – time $= 0.14\,\text{s}$; *C* – time $= 0.21\,\text{s}$; *D* – time $= 0.28\,\text{s}$.

The field of the pressure in the vertical plane of UT-model is presented on the Fig. 3. In the case of a positive rate and acceleration of flow (Fig. 3, *A*) the pattern of pressure is similar to the one from T-model.

When the velocity is maximal (Fig. 2, *B*), pressure has same behavior.

The great difference of the hydrodynamics of flow can be observed in the case of the negative acceleration of the flow in the second part of the systole (Fig. 2, *C*, 2, *D*). At first the pattern of flow on Fig. 3, *C* is similar to one on Fig. 2, *D*. Hence, the negative acceleration will be more if the torsion motion of left ventricle's wall is absent.

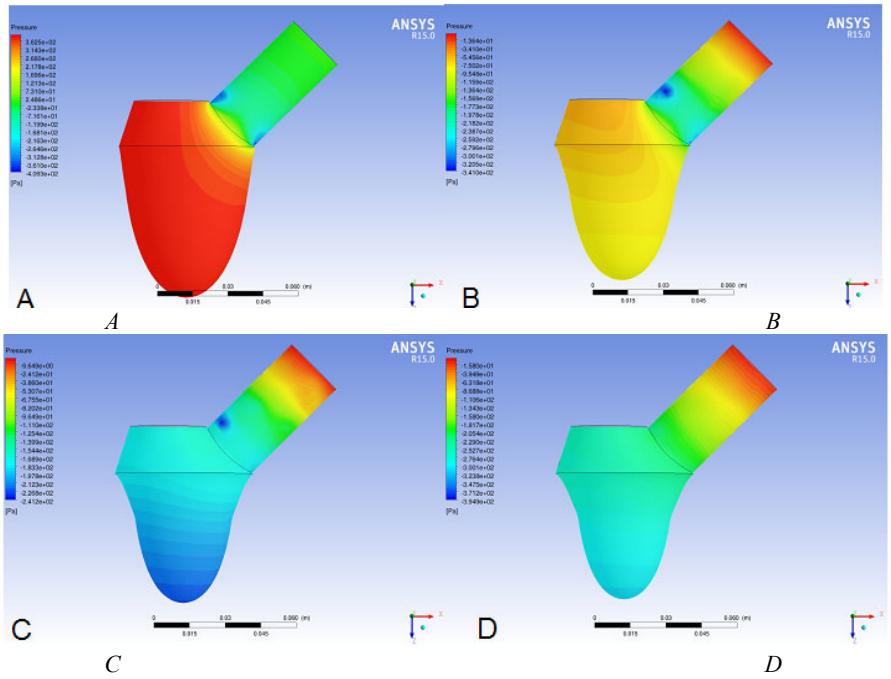

A *B*

C *D*

Fig. 3 – The pressure at the vertical cross plane for UT-models in the different time: *A* – time $= 0.07\,\text{s}$; *B* – time $= 0.14\,\text{s}$; *C* – time $= 0.21\,\text{s}$; *D* – time $= 0.28\,\text{s}$.

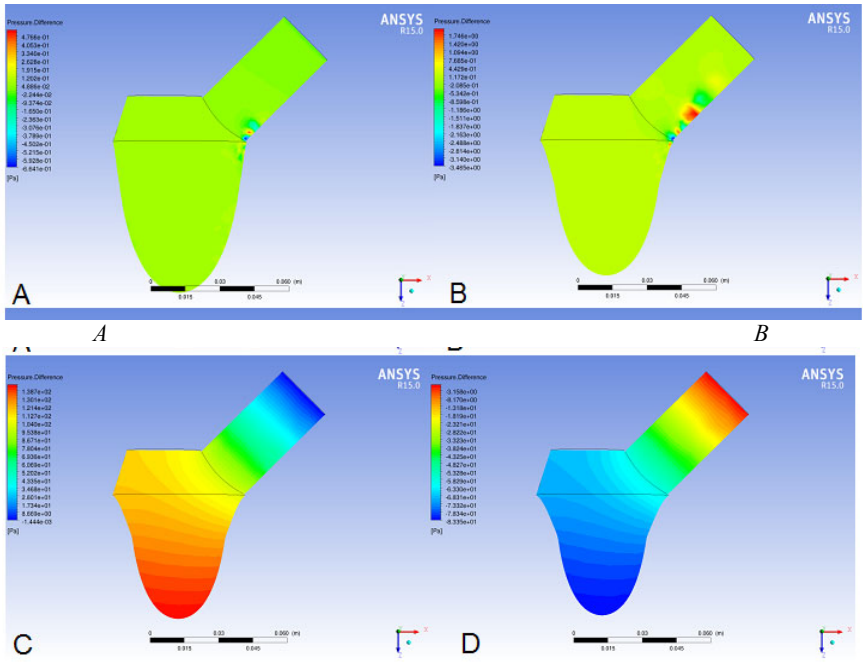

A *B*

C *D*

Fig. 4 – The difference of the pressure at the vertical cross plane for T- model and UT-model in the different time: *A* – time $= 0.07\,\text{s}$; *B* – time $= 0.14\,\text{s}$; *C* – time $= 0.21\,\text{s}$; *D* – time $= 0.28\,\text{s}$.

At the end of systole (Fig. 3, *D*), the pressure has more uniformly type. The consequence is a reduction of a pressure's gradient and a increasing the time of filling of the left ventricle in the diastolic phase of the cardiac circle.

Differences between pressures for T-model and UT-model are present in Fig. 4. We can observe that differences are negligible for the most part of the left ventricle and the ascending aorta excludes bottom part of aorta. In this part, difference is significant. The alterations are nonlinear. We can observe oscillations of the pressure. It proves appearance of the vortex structure in the aorta (Fig. 4, *A*, 4, *B*).

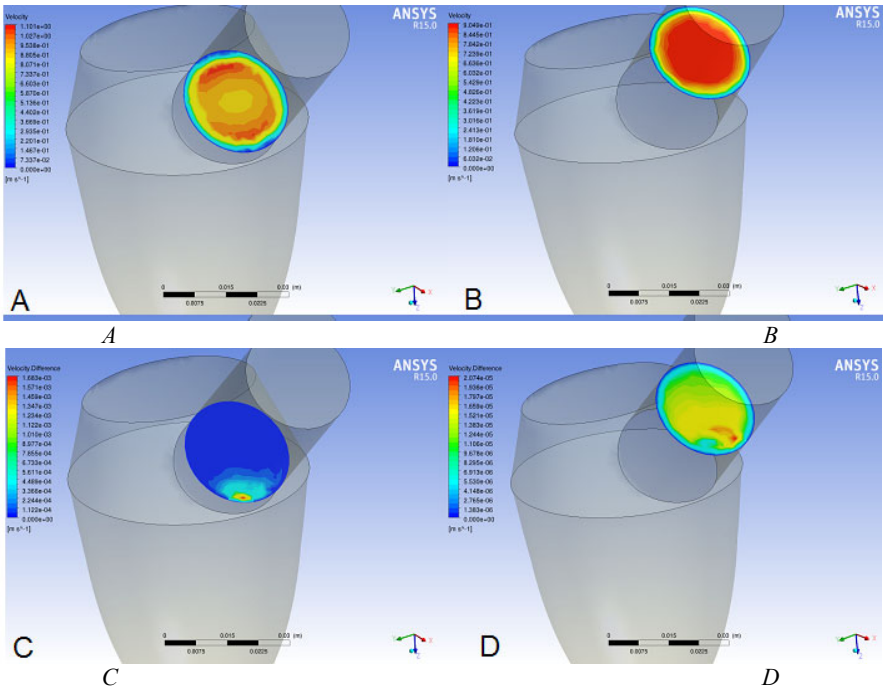

A *B*

C *D*

Fig. 5 – The velocity field at the aorta cross plane for T- models and the difference between data T-model and UT-model, time = 0.07 s :
A – the velocity field at the beginning part of the aortic section; *B* – the velocity field in the middle part of the aortic section;
C – the difference for the beginning part of the aortic section; *D* – the difference for the beginning part of the aortic section.

In the third part oh the systole the gradient of pressure in the direction from the apex to the aorta is higher on the 1 mmHg for T-model. It leads to acceleration of the blood flow throughout the aorta (Fig. 4, *C*). At the end of the systole the negative gradient of the pressure is higher for T-model. Thus the left ventricle is filled more quickly in the diastolic phase of the cardiac circle (Fig. 4, *D*).

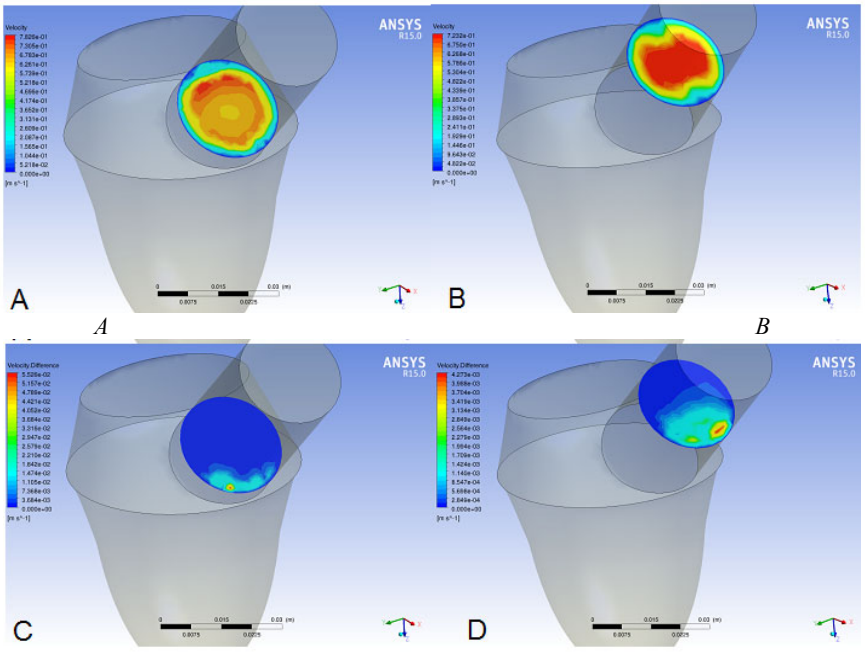

A *B*

C *D*

Fig. 6 – The velocity field at the aorta cross plane for T-models and the difference between data T-model and UT-model, time = 0.14 s :
A – the velocity field at the beginning part of the aortic section; *B* – the velocity field in the middle part of the aortic section;
C – the difference for the beginning part of the aortic section; *D* – the difference for the beginning part of the aortic section.

At the beginning part of the systole the maximum velocity field is located between a core and walls (Fig. 5, *A*). It is a result of a confuser-like flow. The velocity field of middle part look like the straight pipe (Fig. 5, *B*). Differences between velocity's magnitudes are unsignificant and asymmetric.

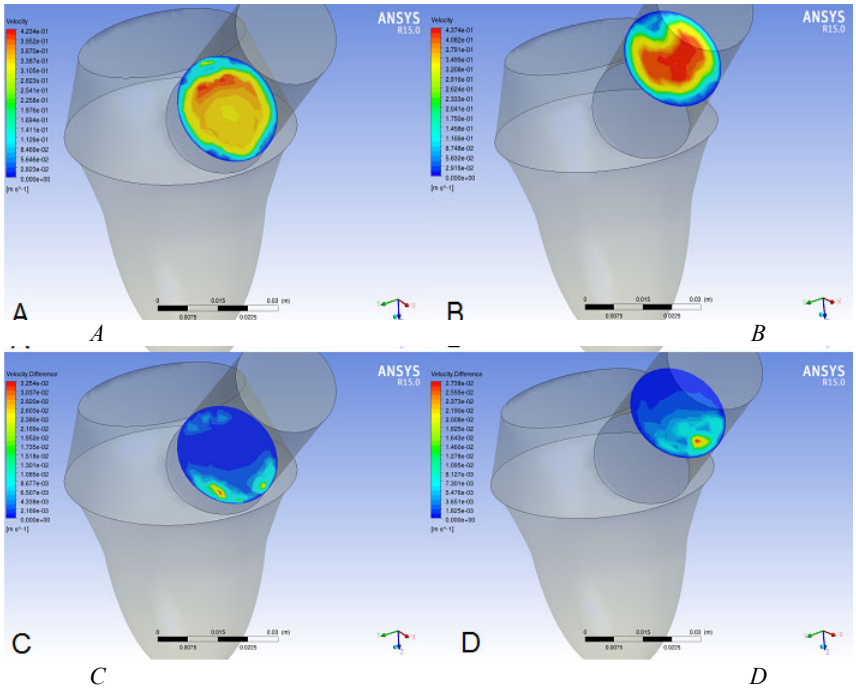

A *B*

C *D*

Fig. 7 – The velocity field at the aorta cross plane for T- models and the difference between data T-model and UT-model, time = 0.21s :
A – the velocity field at the beginning part of the aortic section; *B* – the velocity field in the middle part of the aortic section;
C – the difference for the beginning part of the aortic section; *D* – the difference for the beginning part of the aortic section.

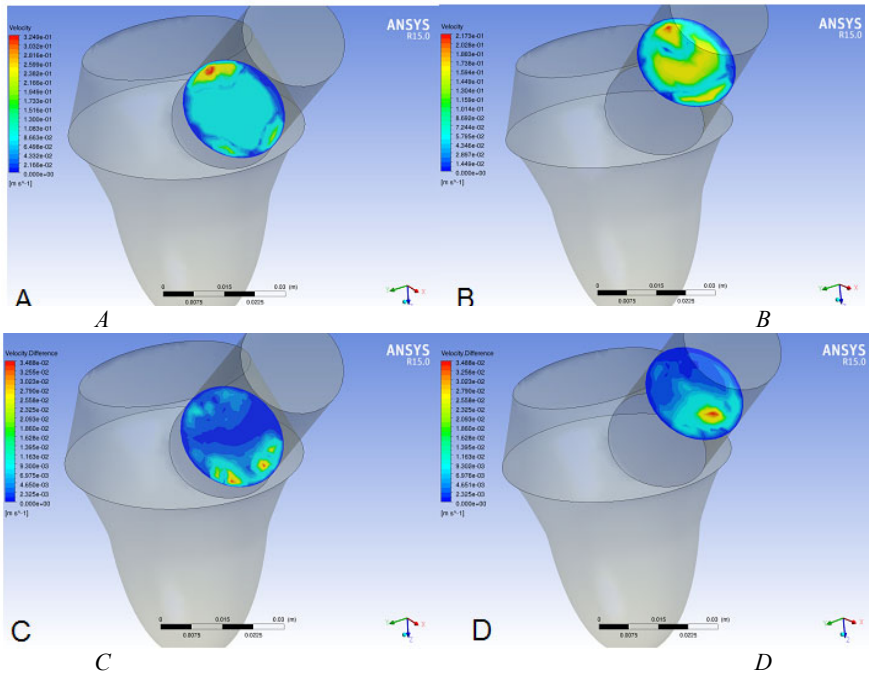

A *B*

C *D*

Fig. 8 – The velocity field at the aorta cross plane for T- models and the difference between data T-model and UT-model, time = 0.28s :
A – the velocity field at the beginning part of the aortic section; *B* – the velocity field in the middle part of the aortic section;
C – the difference for the beginning part of the aortic section; *D* – the difference for the beginning part of the aortic section.

The symmetry of the flow increases in the middle part of the sistole (Fig. 6, *A*, 6, *B*). Differences increase too (Fig. 6, *C*, 6, *D*) and reach 30 % for a small area at the «low-left» part of aorta's root section (Fig. 6, *C*). The pattern of the flow for the middle section has neglecting differences.

The asymmetry increases significantly in the phase of the negative acceleration (Fig. 7, *A*, 7, *B*). The pattern of flow has features for Dean's flow in curved vessels (Fig. 7, *B*). Differences between velocities for T-model and UT-model be-

come more significant (Fig. 7, *C*, 7, *D*), especially at the middle section (Fig. 7, *D*). It is 8 % from velocity's magnitude.

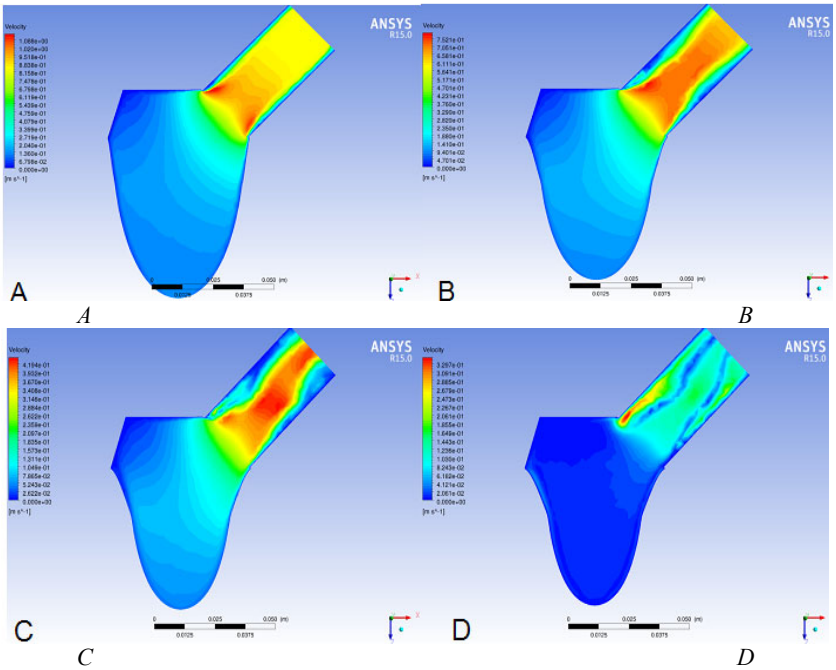

A *B*

C *D*

Fig. 9 – The velocity's field at the vertical cross plane for T- models in the different time: *A* – time $= 0.07\,\text{s}$; *B* – time $= 0.14\,\text{s}$; *C* – time $= 0.21\,\text{s}$; *D* – time $= 0.28\,\text{s}$.

The pattern of the flow is more complicate in the final part of the systole. Secondary flows are more intensive (Fig. 8, *C*, 8, *D*) and differences between velocities for T-model and UT-model are significant for the main part of the cross section as well as aorta's root and the middle section (Fig. 8, *C*, 8, *D*).

The structure of flow is same as for the T-model as for UT-model. We can observe it when compare Fig. 9 and Fig. 10.

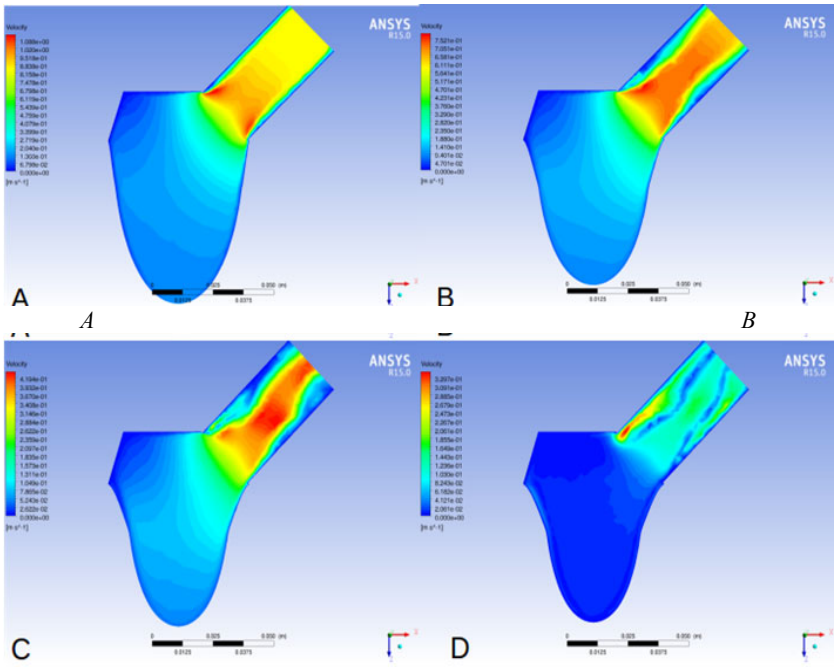

A *B*

C *D*

Fig. 10 – The velocity's field at the vertical cross plane for UT- models in the different time: *A* – time $= 0.07\,\text{s}$; B – time $= 0.14\,\text{s}$; *C* – time $= 0.21\,\text{s}$; *D* – time $= 0.28\,\text{s}$.

The magnitude of the velocity for T-model in the vertical cross section is shown at Fig. 9. The initial phase of the systole is characterized by the main flow. It has the uniform structure for the most part of aortic's domain and has the maximum near the beginning part of the aorta (Fig. 9, *A*). After the flow begins to brake the main flow losses the uni-

form structure and achieves the structure with the maximum of velocity located near the axis of the flow (Fig. 9, *B*). The decreasing the velocity deforms the pattern of the flow and we can observe meandering of the flow (Fig. 9, *C*). The pattern of the flow is very difficult at the final part of the systole and the maximum of velocity relocates to walls of the aorta (Fig. 10, *D*).

But details of velocity's field are really different. Most of differences are located at the wall of the left ventricle for the beginning part of the systole (Fig. 11, *A*). The magnitude of velocity for the T-model significantly higher than for the UT-model at the bottom part of the aorta at next phase (Fig. 11, *B*). The braking of the flow leads to increase the magnitude of the velocity for the T-model for most part of aorta (Fig. 11, *C*). The increasing has a range from 7 % to 10 %. The velocity of the flow decrease but differences don't change. It is a evidence of appearing of a vortex structure (Fig. 11, *D*).

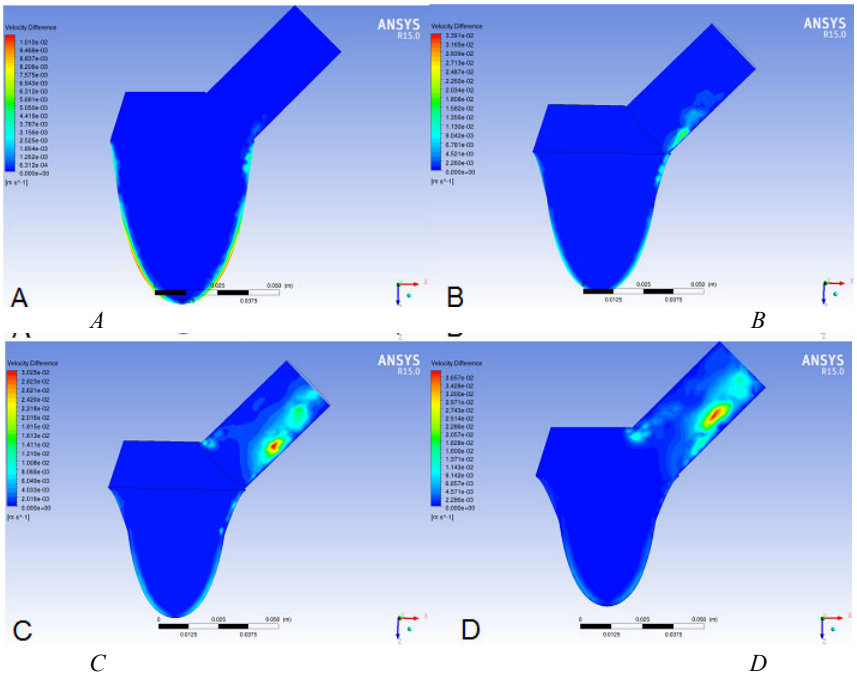

A *B*

C *D*

Fig. 11 – The difference between velocities at the vertical cross plane for T- models and UT-model in the different time:
A – time $= 0.07\,\text{s}$; *B* – time $= 0.14\,\text{s}$; *C* – time $= 0.21\,\text{s}$; *D* – time $= 0.28\,\text{s}$.

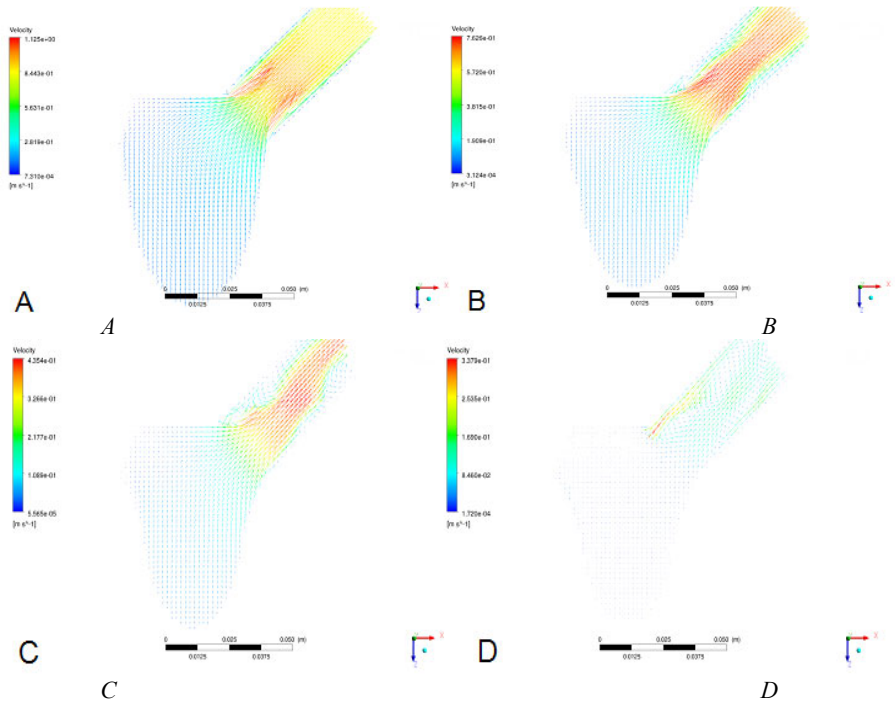

A *B*

C *D*

Fig. 12 – The pressure at the vertical cross plane for T- models in the different time:
A – time $= 0.07\,\text{s}$; *B* – time $= 0.14\,\text{s}$; *C* – time $= 0.21\,\text{s}$; *D* – time $= 0.28\,\text{s}$.

The structure of the flow can be represented with vector plots. In the first half of the systolic phase the pattern of the flow is similar to the common ejection pattern as for the T-model (Fig. 12, *A*, *B*) and for the UT-model (Fig. 13, *A*, *B*). We can observe compression of the flow and the appearing of toroidal vortex in the root part of the aorta (Fig. 12, *A*, 13, *A*). When the acceleration of the flow decreases the vortex spreads along the aorta and the main flow becomes sinuous (Fig. 12, *B*, 13, *B*). The first part of the braking flow is characterized the more complicate vortex structure and creating of the backward flow (Fig. 12, *C*, 13, *C*). The insensitivity of the backward flow dominates in the final part of sistola.

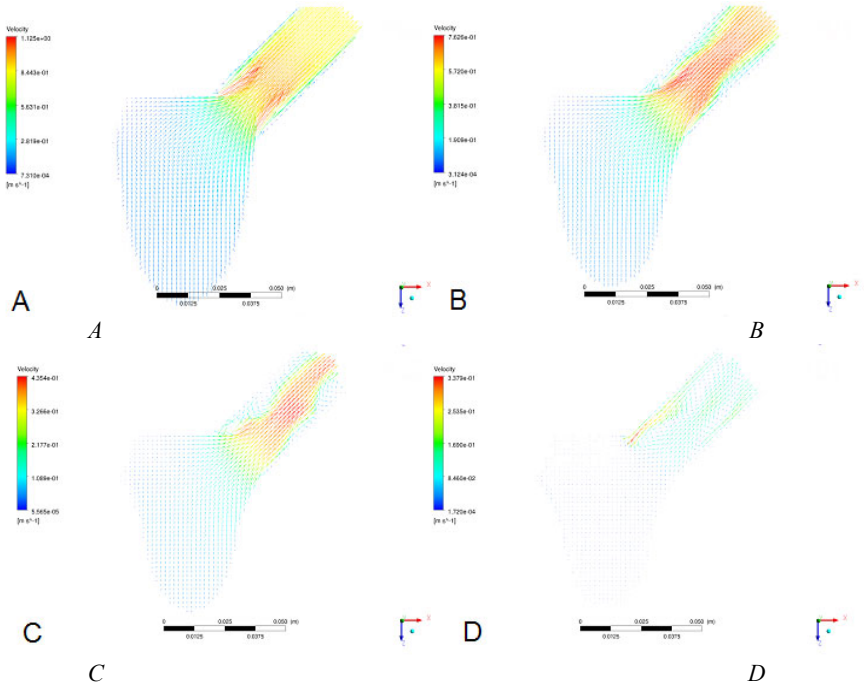

A *B*

C *D*

Fig. 13 – The pressure at the vertical cross plane for UT- models in the different time:
A – time $= 0.07\,\text{s}$; *B* – time $= 0.14\,\text{s}$; *C* – time $= 0.21\,\text{s}$; *D* – time $= 0.28\,\text{s}$.

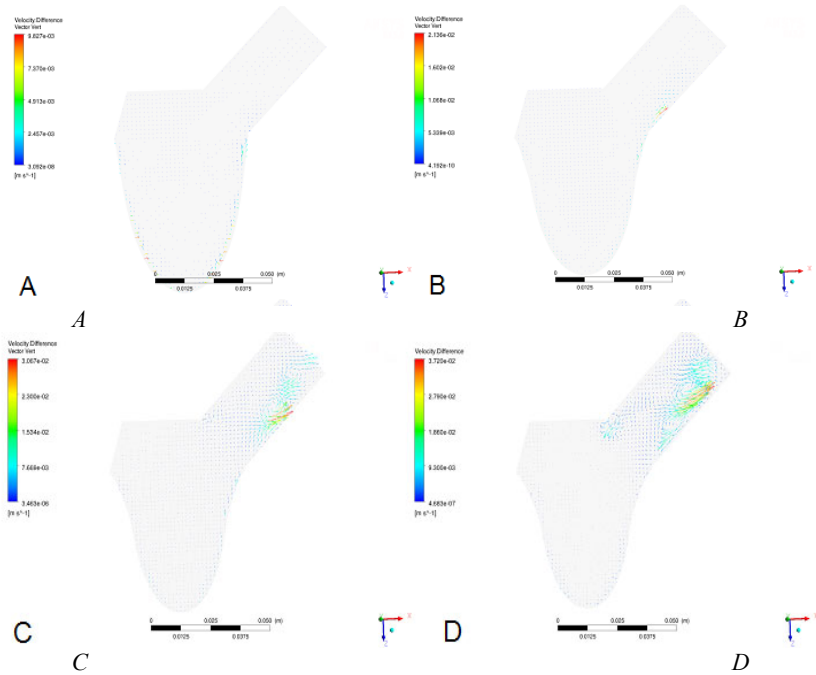

A *B*

C *D*

Fig. 14 – The difference between velocity's magnitudes for T-model and UT- models in the different time:
A – time $= 0.07\,\text{s}$; *B* – time $= 0.14\,\text{s}$; *C* – time $= 0.21\,\text{s}$; *D* – time $= 0.28\,\text{s}$.

Differences between patterns of flow are negligible for the aortic part of the domain and significant near left ventricle's wall of the beginning part of systole (Fig. 14, *A*). The decreasing of the flow shifts the area with great differences to the aorta (Fig. 14, *B*). In the beginning phase of the braking flow we can observe great differences between models. Tor-

sion motion is a cause of more intensive rotate motion in aorta (Fig. 14, *C*). Moreover, the vortex structure for the T-model is more complicate then the pattern of the flow for the UT-model. Differences spread in a backward direction (from the aorta to the ventricle) in the last part of systole (Fig. 14, *D*).

Conclusion. We can note that torsional motion influences to the pattern of flow in the left ventricle. It creates the condition for more quick filling of the left ventricle because the gradient of the pressure significantly greater. The disturbance of torsional motion leads to deterioration of blood circulation and correspondingly decreasing oxigenation.

To fully understand the physiological principles of left ventricular torsion (LV torsion), further research is needed. Despite significant technical limitations, considerable knowledge has already been gained regarding left ventricular rotation in a healthy heart. However, only a single calculation method that describes rotation as an angular displacement around the circumference and along the longitudinal axis throughout the entire cardiac cycle and adjusts for centroid motion will enable the use of left ventricular torsion as a measure for the quantitative assessment of myocardial dysfunction associated with a wide range of heart diseases. Since the amount and timing of left ventricular torsion are directly related to the structure and function of the myocardium and cardiomyocytes, left ventricular torsion represents a promising measure for the qualitative as well as quantitative detection of (sub)clinical (systolic and diastolic) dysfunction.

This work was partially supported by a grant from the Simons Foundation (Award 1160640, Presidential Discretionary-Ukraine Support Grants, Vitalii Overko).

Bibliography

1. *Fyrenius A*., *Wigström L*., *Ebbers T*., *Karlsson M*., *Engvall J*., *Bolger A*. Three dimensional flow in the human left atrium // Heart (British Cardiac Society). – 2001. – vol. 86(4). – P. 448 – 455. DOI: 10.1136/heart.86.4.448.
2. *Kilner P. J*., *Yang G.-Z*., *Wilkes A. J*., *Mohiaddin R. H*., *Firmin D. N*., *Yacoub M. H*. Asymmetric redirection of flow through the heart // Nature. – 2000. – vol. 404(6779). – P. 759 – 764. DOI: 10.1038/35008075.
3. *Tanne D*., *Bertrand E*., *Pibarot P*., *Rieu R*. Asymmetric flows in an anatomical-shaped left atrium by 2C-3D+T PIV measurements // Computer Methods in Biomechanics and Biomedical Engineering. – COMPUT METHODS BIOMECH BIOMED, 2008. – vol. 11. – P. 209 – 211. DOI: 10.1080/10255840802298943.
4. *Helle-Valle T*., *Crosby J*., *Edvardsen T*., *Lyseggen E*., *Amundsen B. H*., *Smith H. J*., *Rosen B. D*., *Lima J. A*., *Torp H*., *Ihlen H*., *Smiseth O. A*. New noninvasive method for assessment of left ventricular rotation: speckle tracking echocardiography // Circulation. – 2005. – vol. 112. – P. 3149–3156. DOI: 10.1161/CIRCULATIONAHA.104.531558.
5. *McDonald I. G*. The shape and movements of the human left ventricle during systole: a study by cineangiography and by cineradiography of picardial markers // The American journal of cardiology. – 1970. – vol. 26(3). – P. 221 – 230. DOI: 10.1016/0002-9149(70)90787-3.
6. *Rademakers F. E*., *Buchalter M. B*., *Rogers W. J*., *Zerhouni E. A*., *Weisfeldt M. L*., *Weiss J. L*., *Shapiro E. P*. Dissociation between left ventricular untwisting and filling: accentuation by catecholamines // Circulation. – 1992. – vol. 85(4). – P. 1572 – 1581. DOI: 10.1161/01.cir.85.4.1572.
7. *Gibbons Kroeker C. A*., *Ter Keurs H. E*., *Knudtson M. L*., *Tyberg J. V*., *Beyar R*. An optical device to measure the dynamics of apex rotation of the left ventricle // The American journal of physiology. – 1993. – vol. 265(4 Pt 2). – H1444 – H1449. DOI: 10.1152/ajpheart.1993.265.4.H1444.
8. *Moon M. R*., *Ingels N. B. Jr*., *Daughters G. T*., *Stinson E. B*., *Hansen D. E*., *Miller D. C*. Alterations in left ventricular twist mechanics with inotropic stimulation and volume loading in human subjects // Circulation. – 1994. – vol. 89(1). – P. 142 – 150. DOI: 10.1161/01.cir.89.1.142.
9. *Hansen D. E*., *Daughters G. T*., *Alderman E. L*., *Ingels N. B*., *Stinson E. B*., *Miller D. C*. Effect of volume loading, pressure loading, and inotropic stimulation on left ventricular torsion in humans // Circulation. – 1991. – vol. 83(4). – P. 1315 – 1326. DOI: 10.1161/01.cir.83.4.1315.
10. *Notomi Y*., *Lysyansky P*., *Setser R. M*., *Shiota T*., *Popović Z. B*., *Martin-Miklovic M. G*., *Weaver J. A*., *Oryszak S. J*., *Greenberg N. L*., *White R. D*., *Thomas J. D*. Measurement of ventricular torsion by two-dimensional ultrasound speckle tracking imaging // Journal of the American College of Cardiology. – 2005. – vol. 45(12). – P. 2034 – 2041. DOI: 10.1016/j.jacc.2005.02.082.
11. *Issa R*. Solution of the implicitly discretised fluid flow equations by operator-splitting // Journal of Computational Physics. – 1986. – Vol. 62. – no. 1. – P. 40 – 65. DOI: 10.1016/0021-9991(86)90099-9.
12. *Stefanou K*., *Naka K*., *Michalis L*., *Filipović N*., *Parodi O*. Blood flow in arterial segments: Rigid vs. deformable walls simulations // J. Serbian Soc. Comput. Mech. – 2011. – vol. 5. – pp. 69 – 77.
13. *Shibeshi S. S*., *Collins W. E*. The rheology of blood flow in a branced arterial system // Applied rheology (Lappersdorf, Germany: Online). – 2005. – vol. 15(6). – pp. 398 – 405. DOI: 10.1901/jaba.2005.15-398.
14. *Gharahi H*., *Zambrano B. A*., *Zhu D. C*., *DeMarco J. K*., *Baek S*. Computational fluid dynamic simulation of human carotid artery bifurcation based on anatomy and volumetric blood flow rate measured with magnetic resonance imaging // International journal of advances in engineering sciences and applied mathematics. – 2016. – vol. 8(1). – pp. 46 – 60. DOI: 10.1007/s12572-016-0161-6.
15. *Olufsen M. S*. A one-dimensional fluid dynamic model of the systemic arteries // Stud. Health Technol. Inform. – 2000. – vol. 71. – pp. 79 – 97. PMID: 10977605.
16. *Johnston B. M*., *Johnston P. R*., *Corney S*., *Kilpatrick D*. Non-Newtonian blood flow in human right coronary arteries: Steady state simulations // J. Biomech. – 2004. – vol. 37. – pp. 709 – 720. DOI: 10.1016/j.jbiomech.2003.09.016.
17. *Bell J. B*., *Colella P*., *Glaz H. M*. Second-Order Projection Method for the Incompressible Navier-Stokes Equations // J. Comput. Phys. – 1989. – vol. 283. – pp. 257 – 283. DOI: 10.1016/0021-9991(89)90151-4.
18. *Sigrid Kaarstad Dahl*. Numerical Simulations of Blood Flow in the Left Side of the Heart. Thesis for the degree of Philosophiae Doctor Trondheim. – Norwegian University of Science and Technology, 2012. – 118 p.
19. *Watanabe H*., *Sugiura S*., *Kafuku H*., *Hisada T*. Multiphysics simulation of left ventricular filling dynamics using fluid-structure interaction finite element method // Biophysical journal. – 2004. – Vol. 87(3). – pp. 2074 – 2085. DOI: 10.1529/biophysj.103.035840.

References (transliterated)

1. Fyrenius A., Wigström L., Ebbers T., Karlsson M., Engvall J., Bolger A. Three dimensional flow in the human left atrium. *Heart (British Cardiac Society)*. 2001, vol. 86(4), pp. 448–455. DOI: 10.1136/heart.86.4.448.
2. Kilner P. J., Yang G.-Z., Wilkes A. J., Mohiaddin R. H., Firmin D. N., Yacoub M. H. Asymmetric redirection of flow through the heart. *Nature*. 2000, vol. 404(6779), pp. 759–764. DOI: 10.1038/35008075.
3. Tanne D., Bertrand E., Pibarot P., Rieu R. Asymmetric flows in an anatomical-shaped left atrium by 2C-3D+T PIV measurements. *Computer*

Methods in Biomechanics and Biomedical Engineering. COMPUT METHODS BIOMECH BIOMED, 2008, vol. 11, pp. 209–211. DOI: 10.1080/ 10255840802298943.

4. Thomas Helle-Valle, Jonas Crosby, Thor Edvardsen, Erik Lyseggen, Brage H. Amundsen, Hans-Jørgen Smith, Boaz D. Rosen, João A.C. Lima, Hans Torp, Halfdan Ihlen, Otto A. Smiseth. New Noninvasive Method for Assessment of Left Ventricular Rotation. *Circulation*. 2005, 112:3149–3156. DOI: 10.1161/ CIRCULATIONAHA.104.531558.
5. McDonald I. G. The shape and movements of the human left ventricle during systole: a study by cineangiography and by cineradiography of picardial markers. *The American journal of cardiology*. 1970, vol. 26(3), pp. 221–230. DOI: 10.1016/0002-9149(70)90787-3.
6. Rademakers F. E., Buchalter M. B., Rogers W. J., Zerhouni E. A., Weisfeldt M. L., Weiss J. L., Shapiro E. P. Dissociation between left ventricular untwisting and filling: accentuation by catecholamines. *Circulation*. 1992, vol. 85(4), pp. 1572–1581. DOI: 10.1161/01.cir.85.4.1572.
7. Gibbons Kroeker C. A., Ter Keurs H. E., Knudtson M. L., Tyberg J. V., Beyar R. An optical device to measure the dynamics of apex rotation of the left ventricle. *The American journal of physiology*. 1993, vol. 265(4 Pt 2), H1444 –H1449. DOI: 10.1152/ajpheart.1993.265.4.H1444.
8. Moon M. R., Ingels N. B. Jr., Daughters G. T., Stinson E. B., Hansen D. E., Miller D. C. Alterations in left ventricular twist mechanics with inotropic stimulation and volume loading in human subjects. *Circulation*. 1994, vol. 89(1), pp. 142–150. DOI: 10.1161/01.cir.89.1.142.
9. Hansen D. E., Daughters G. T., Alderman E. L., Ingels N. B., Stinson E. B., Miller D. C. Effect of volume loading, pressure loading, and inotropic stimulation on left ventricular torsion in humans. *Circulation*. 1991, vol. 83(4), pp. 1315–1326. DOI: 10.1161/01.cir.83.4.1315.
10. Notomi Y., Lysyansky P., Setser R. M., Shiota T., Popović Z. B., Martin-Miklovic M. G., Weaver J. A., Oryszak S. J., Greenberg N. L., White R. D., Thomas J. D. Measurement of ventricular torsion by two-dimensional ultrasound speckle tracking imaging. *Journal of the American College of Cardiology*. 2005, vol. 45(12), pp. 2034–2041. DOI: 10.1016/j.jacc.2005.02.082.
11. Issa R. Solution of the implicitly discretised fluid flow equations by operator-splitting. *Journal of Computational Physics*. 1986, Vol. 62, no. 1, pp. 40–65. DOI: 10.1016/0021-9991(86)90099-9.
12. Stefanou K., Naka K., Michalis L., Filipović N., Parodi O. Blood flow in arterial segments: Rigid vs. deformable walls simulations. *J. Serbian Soc. Comput. Mech*. 2011, vol. 5, pp. 69–77.
13. Shibeshi S. S., Collins W. E. The rheology of blood flow in a branced arterial system. *Applied rheology (Lappersdorf, Germany: Online)*. 2005, vol. 15(6), pp. 398–405. DOI: 10.1901/jaba.2005.15-398.
14. Gharahi H., Zambrano B. A., Zhu D. C., DeMarco J. K., Baek S. Computational fluid dynamic simulation of human carotid artery bifurcation based on anatomy and volumetric blood flow rate measured with magnetic resonance imaging. *International journal of advances in engineering sciences and applied mathematics*. 2016, vol. 8(1), pp. 46–60. DOI: 10.1007/s12572-016-0161-6.
15. Olufsen M. S. A one-dimensional fluid dynamic model of the systemic arteries. *Stud. Health Technol. Inform*. 2000, vol. 71, pp. 79–97. PMID: 10977605.
16. Johnston B. M., Johnston P. R., Corney S., Kilpatrick D. Non-Newtonian blood flow in human right coronary arteries: Steady state simulations. *J. Biomech*. 2004, vol. 37, pp. 709–720. DOI: 10.1016/j.jbiomech.2003.09.016.
17. Bell J. B., Colella P., Glaz H. M. Second-Order Projection Method for the Incompressible Navier-Stokes Equations. *J. Comput. Phys*. 1989, vol. 283, pp. 257–283. DOI: 10.1016/0021-9991(89)90151-4.
18. Sigrid Kaarstad Dahl. *Numerical Simulations of Blood Flow in the Left Side of the Heart. Thesis for the degree of Philosophiae Doctor Trondheim*. Norwegian University of Science and Technology, 2012. 118 p.
19. Watanabe H., Sugiura S., Kafuku H., Hisada T. Multiphysics Simulation of Left Ventricular Filling Dynamics Using Fluid-Structure Interaction Finite Element Method. *Biophysical Journal*. 2004, Vol. 87(3), pp. 2074–2085. DOI: 10.1529/biophysj.103.035840.

Надійшла (received) 25.05.2025

Відомості про авторів / Information about authors

Оверко Віталій Станіславович – молодший науковий співробітник, Інститут прикладної математики та механіки НАН України, м. Черкаси; тел.: (093) 013-82-05; ORCID: https://orcid.org/0000-0002-4861-3274; e-mail: vitaliiverko@gmail.com.

Overko Vitalii Stanislavovych – Junior Researcher, Institute of Applied Mathematics and Mechanics NAS Ukraine, Cherkasy; tel.: (093) 013-82-05; ORCID: https://orcid.org/0000-0002-4861-3274; e-mail: vitaliiverko@gmail.com.